Interaction of apolipoprotein A-I in three different conformations with palmitoyl oleoyl phosphatidylcholine vesicles

M. Alejandra Tricerri,* Susana A. Sanchez,† Cristina Arnulphi,* Diane M. Durbin,* Enrico Gratton,† and Ana Jonas[1],*

Department of Biochemistry,* and Laboratory for Fluorescence Dynamics,† University of Illinois at Urbana-Champaign, Urbana, IL 61801

Abstract **Interactions of apolipoprotein A-I (apoA-I) with cell membranes appear to be important in the initial steps of reverse cholesterol transport. The objective of this work was to examine the effect of three distinct conformations of apoA-I (lipid-free and in 78 Å or 96 Å reconstituted high density lipoproteins, rHDL) on its ability to bind to, and abstract lipids from, palmitoyl oleoyl phosphatidylcholine membrane vesicles (small unilamellar vesicles, SUV, and giant unilamellar vesicles, GUV). The molecular interactions were observed by two-photon fluorescence microscopy, and the binding parameters were quantified by gel-permeation chromatography or isothermal titration microcalorimetry. Rearrangement of apoA-I-containing particles after exposure to SUVs was examined by native gel electrophoresis. The results indicate that lipid-free apoA-I binds reversibly, with high affinity, to the vesicles but does not abstract a significant amount of lipid nor perturb the vesicle structure. The 96 Å rHDL, where all the amphipathic helices of apoA-I are saturated with lipid within the particles, do not bind to vesicles or perturb their structure. In contrast, the 78 Å rHDL have a region of apoA-I, corresponding to a few amphipathic helical segments, which is available for external or internal phospholipid binding. These particles bind to vesicles with measurable affinity (lower than lipid-free apoA-I), abstract lipids from the membranes, and form particles of larger diameters, including 96 Å rHDL. We conclude that the conformation of apoA-I regulates its binding affinity for phospholipid membranes and its ability to abstract lipids from the membranes.**—Tricerri, M. A., S. A. Sanchez, C. Arnulphi, D. M. Durbin, E. Gratton, and A. Jonas. **Interaction of apolipoprotein A-I in three different conformations with palmitoyl oleoyl phosphatidylcholine vesicles.** ***J. Lipid Res.*** **2002.** 43: **187–197.**

Supplementary key words vesicle interactions • small unilamellar vesicles • giant unilamellar vesicles • remodeling of HDL

Extensive epidemiological research and recent experimental studies with transgenic animals support an important role of HDL and their major protein component, apolipoprotein A-I (apoA-I), in the protection against coronary heart disease (CHD) (1–3). A key mechanism in the prevention of atherosclerosis by HDL is its ability to remove cholesterol and phospholipids from cells, initiating the reverse cholesterol transport (RCT) process, by which cholesterol is carried from the peripheral tissues to the liver for excretion and further metabolism (4, 5). ApoA-I determines and regulates the functions of HDL in several ways: *1*) as activator of the LCAT reaction in plasma (6), *2*) as acceptor of cellular cholesterol and phospholipids from cells (7, 8), and *3*) as a carrier of the LCAT-derived cholesteryl esters to the liver by its interaction with the SR-BI receptor (9). The HDL fraction in human plasma is highly heterogeneous, with particles differing in composition, size, density, and shape (10). There is increasing evidence that apoA-I can adopt many distinct conformations, and that its ability to rearrange in response to changes in HDL lipids due to the action of plasma factors, play a key role in modulating the functions of the different HDL subpopulations (11, 12). Because of their participation in reverse cholesterol transport, attention has turned to nascent subspecies of HDL containing apoA-I as its sole protein moiety. These HDL with preβ migration on agarose gels were isolated from lymph (13) and plasma (14), and sepa-

Abbreviations: Alexa 488, Alexa Fluor 488 carboxylic acid, succinimidyl ester, di lithium salt; apoA-I, apolipoprotein A-I; ε, molar extinction coefficient; ^{3}H-DPPC, L-α-dipalmitoyl, [2-palmitoyl-9,10-^{3}H(N)] phosphatidylcholine; GndHCl, guanidine hydrochloride; GUV, giant unilamellar vesicles; ITC, isothermal titration microcalorimetry; LAURDAN, 6-dodecanoyl-2-dimethylaminonaphthalene; PC, phosphatidylcholine; POPC, 1-palmitoyl,2-oleoyl phosphatidylcholine; rHDL, reconstituted HDL; RCT, reverse cholesterol transport; SUV, small unilamellar vesicles.

[1] To whom correspondence should be addressed at Department of Biochemistry, College of Medicine at Urbana-Champaign, University of Illinois, 506 Matthews Ave., Urbana, IL 61801.
e-mail: a-jonas@uiuc.edu

rated into three main subfractions according to their size and composition (15). The smallest of the preβ-HDL, the lipid poor preβ$_1$-HDL particles, are the initial acceptors of cellular cholesterol. Later the cholesterol is channeled to the large preβ$_3$-HDL where it is esterified and then transferred to α-HDL (15, 16).

The molecular basis for the ability of nascent HDL to take up cholesterol from cells is not yet clear. In fact, several mechanisms could be contributing to the process: *1*) spontaneous aqueous diffusion of cholesterol from cell membranes to the HDL particles, *2*) interaction of apoA-I with membrane lipid domains and microsolubization of phospholipids and cholesterol, and *3*) specific apolipoprotein interactions with the plasma membrane transporter ABC1 (8) or SR-BI receptors, which facilitate lipid efflux from cells (17, 18).

In this study we set out to examine the second process: the interaction of lipid-free apoA-I or lipid-bound apoA-I in reconstituted high density lipoprotein (rHDL) particles with phospholipid membranes. To facilitate the interpretation of the results, we selected well-defined model systems: reconstituted HDL for the nascent HDL subspecies and two vesicle preparations for the cellular membranes. Reconstituted, discoidal HDL having two apoA-I molecules per particle, and different phospholipid contents, are particularly useful models due to their similarity to the natural nascent HDL (preβ-HDL) secreted in vivo by the liver and intestine, or produced during catabolism of other circulating lipoproteins (19). The rHDL selected for this study have well-defined diameters (78 and 96 Å), distinct apoA-I conformations (20), and dramatically different functional properties as reflected in their activation of LCAT (21) and binding affinity for SR-BI receptor (22). Therefore, we hypothesize that these rHDL particles, with distinct functional properties in the middle and final steps of RCT, may also exhibit differential behavior in the first step of the process—interaction with membranes. Further, we propose that the reversible conformational changes in the apoA-I components of these particles serve as molecular switches that regulate the behavior of the HDL subspecies in RCT.

As models for cell membranes, we chose the well-studied small unilamellar vesicles (SUV) of phosphatidylcholines (23), which researchers have used for over 30 years in the study of the interactions of proteins with phospholipid bilayers in aqueous solutions (24). Although especially useful in quantitative binding studies and biochemical analysis of the interaction products, the SUVs have a high surface curvature, unequal packing of phospholipids in the outer and inner leaflets of the bilayer, and slightly altered phase transition behavior compared with planar phospholipid bilayers. All of these factors could affect interactions with proteins (25). Thus we also used a novel system, giant unilamellar vesicles (GUV), which represents a more realistic model for cell membranes (26), in conjunction with two-photon fluorescence microscopy (27), to visualize directly and in real-time the interaction of apoA-I, and the rHDL containing apoA-I, with membranes.

MATERIALS AND METHODS

Materials

Human apoA-I was purified from blood plasma purchased from the Champaign County Blood Bank, Regional Health Center, as described previously (28). Fluorescamine, 1-palmitoyl, 2-oleoyl phosphatidylcholine (POPC) and sodium cholate were purchased from Sigma Chemical Co. (St. Louis, MO); ultrapure guanidine hydrochloride (GndHCl) was obtained from Boehringer Mannheim. The Alexa Fluor 488 protein labeling kit and 6-dodecanoyl-2-dimethylaminonaphthalene (LAURDAN) were purchased from Molecular Probes (Eugene, OR); [^{3}H]DPPC (92.3 Ci/mmol) was from Du Pont (NEN, MA). Bis(sulfosuccinimidyl)suberate (BS^3) was purchased from Pierce (Rockford, IL). MOPS and dichloromethane were from Fisher Scientific (Springfield, NJ).

Methods

Labeling of apoA-I. ApoA-I (2–4 mg) in 0.1 M sodium bicarbonate, pH 8.3, was incubated with Alexa 488 (dissolved in the same buffer) at a molar ratio of probe to protein of 30:1. After 2 h incubation, in the dark at room temperature, unreacted probe was separated by elution through a PD-10 column (Pharmacia, Peapack, NJ), followed by overnight dialysis against 10 mM TBS, pH 8.0, 0.15 M NaCl, 1 mM NaN_3, and 0.1 mM EDTA. The degree of labeling of amino groups in apoA-I was determined from absorbance measurements on the conjugate at 280 nm (ε_{280} = 7,800 M^{-1} for the probe and ε_{280} = 30,700 M^{-1} for apoA-I) and at 492 nm (ε_{492} = 71,000 M^{-1} for Alexa-488) (29). Under these conditions, the efficiency of labeling was about one molecule of probe per molecule of apoA-I. Reconstituted HDL containing labeled apoA-I was prepared in high yields, as described below.

Preparation of reconstituted discoidal HDL. rHDL, having two molecules of apoA-I per particle, were prepared by the sodium cholate dialysis method (30). A starting molar ratio of POPC-protein-sodium cholate, 95:1:150 (v/v/v) was used in order to obtain 96 Å rHDL. The desired amount of POPC in $CHCl_3$ was dried under N_2. Lipids were dispersed in TBS and sodium cholate was added and kept at 4°C until the lipid dispersion cleared. Proteins were incubated 30 min with the mixed micelles and the mixtures were dialyzed extensively against TBS at 4°C. When necessary, preparations were passed through a Superdex 200 HR 10/30 column (Pharmacia FPLC System) equilibrated with the same buffer at a flow rate of 0.25 ml/min. The smaller 78 Å rHDL were reconstituted from a starting molar ratio of POPC-apoA-I-sodium cholate of 35:1:60 (v/v/v) using the same procedure. Fractions that were free of higher molecular weight complexes after the first column elution were concentrated and further purified by a second chromatographic step. For this step, the same column was equilibrated with TBS plus 0.1 M GndHCl, and a flow rate of 0.4 ml/min was used. The small amount of GndHCl was included to facilitate removal of lipid-free apoA-I. After the elution, pure fractions were dialyzed against TBS. The homogeneity and hydrodynamic diameters of the rHDL were estimated by native (8–25%) polyacrylamide gradient gel electrophoresis on a Pharmacia Phast System. Protein was quantified either by absorbance at 280 nm, or by a modified Lowry assay (31). Phospholipid content was determined by phosphorus analysis according to Chen et al. (32). Chemical cross-linking with BS^3 of the apoA-I on the rHDL was performed as described by Leroy et al. (33).

Giant unilamellar vesicles. Giant unilamellar vesicles were prepared, at least twice, as described by Bagatolli et al. (34). To prepare the GUVs, ~2 μl of POPC stock solution (0.2 mg/ml in $CHCl_3$) were spread onto two platinum wires in a small chamber

under a stream of N_2. To remove residual organic solvent, samples were dried under vacuum for about 30 min. The bottom of the chamber was sealed with a coverslip and the dry sample chamber was then filled with ~2 ml of 1 mM Tris pH 8.0 buffer at room temperature. Immediately after this step, the platinum wires were connected to a function generator (Hewlett-Packard, Santa Clara, CA), and a low frequency AC field (sinusoidal wave function with a frequency of 10 Hz and an amplitude of 3 V) was applied for 1 h. A CCD color video camera (CCD-Iris, Sony) connected to the microscope was used to follow the vesicle formation and to select the target vesicle for analysis. The vesicles remaining attached to the platinum wires were used for the observations; they were stable for at least 2 h.

In the two-photon excitation process, a fluorophore absorbs two photons simultaneously, each of them supplying half of the required energy for the electronic transition. This approach provides several advantages over the traditional confocal microscopy: *1*) due to the long excitation wavelength (780 nm) there is no overlap between the excitation and emission spectra, *2*) photobleaching and photodamage above and below the focal plane is minimal, and *3*) in order to obtain the high photon densities required for two-photon absorption, a high-peak power laser light source is focused on a diffraction-limited spot through a high numerical aperture objective. As a consequence, there is no light absorption in the areas above and below the focal plane, allowing a sectioning effect without the use of pinholes (27). The observations were carried out using an inverted microscope (Axiovert 35, Zeiss, Thornwood, NY). An LD-Achroplan20× long working distance air objective (Zeiss, Holmdale, NJ), with a numerical aperture of 0.4, was used in the microscope. A titanium-sapphire laser (Mira 900, Coherent, Palo Alto, CA) pumped by a frequency-doubled Nd:vanadate laser (Verdi, Coherent), was used as the excitation light source. The laser was guided by a galvanometer-driven x-y scanner (Cambridge Technology, Watertown, MA). The scanning rate was controlled by the input signal from a frequency synthesizer (Hewlett-Packard, Santa Clara, CA), and a frame rate of 9 s was used to acquire the images (256 × 256 pixels). To change the polarization of the laser light from linear to circular, a quarter wave plate (CVI Laser Corporation, Albuquerque, NM) was placed after the polarizer. The fluorescence emission was observed through a broad band-pass filter from 350 to 600 nm (BG39 filter, Chroma Technology, Brattleboro, VT).

Two general procedures were followed in the acquisition of two-photon fluorescence images. *1*) For the binding experiments, 5 μg of Alexa-labeled apoA-I (in the lipid-free state or in 78 or 96 Å rHDL) were added to the unlabeled vesicles. Two-photon imaging required integration of at least 80 frames due to the low fluorescence intensity. The comparative binding between the different samples was estimated by obtaining the horizontal intensity profile on each image, and integrating the area under the curve of the peak corresponding to the protein associated with the membrane. *2*) To observe morphological changes on the vesicle surface, 1 μl of LAURDAN in dimethyl sulfoxide (DMSO) was added to the chamber after the vesicle formation (final LAURDAN to lipid molar ratio 1:100), and left to stabilize for about 15 min. Then, 5 μg of unlabeled apoA-I in the three states were added to the vesicles and images were recorded at room temperature over 2 h. The fluorescence of the LAURDAN was sufficiently bright to obtain good images from single frame measurements. Experiments were repeated, with equivalent results, for two preparations of lipid-free apoA-I and the rHDL particles.

Small unilamellar vesicles. To prepare small unilamellar vesicles (SUVs) of diameters in the range from 250–300 Å, about 60 mg of POPC (dissolved in $CHCl_3$) were combined with a trace amount of [^{3}H]-DPPC to a specific radioactivity of about 90 cpm/μg phospholipid. Lipids were dried under N_2 and under vacuum to remove any traces of solvent, and were resuspended slowly in 5 ml of 0.025 M 3-(*N*-morpholino) propane-sulfonic acid (MOPS), 0.16 M potassium chloride, pH 7.4 (MOPS buffer) to obtain a milky dispersion of multilamellar liposomes (MLV). The suspension was placed on ice under a flow of N_2 and sonicated (amplitude 35%) on a Vibra Cell VCX-400 using a microprobe (Sonics, CT), until the solution became translucent. The preparation was filtered to remove titanium debris and eluted on a 60 × 1.5 cm Superose CL-4B column (Pharmacia), equilibrated with MOPS buffer. Radioactivity in the eluted fractions was detected and quantified by liquid scintillation counting. Typically, some large vesicles came through in the excluded volume and SUVs eluted as a single symmetrical peak. Fractions corresponding to homogeneous SUV were pooled and concentrated to ~16 mg POPC/ml.

For isothermal titration microcalorimetry (ITC) experiments, liposomes were prepared using the same technique with minor modifications: POPC (from a $CHCl_3$ stock) was dried under N_2, then it was dissolved in dichloromethane in order to remove traces of ethanol, which is frequently used to stabilize $CHCl_3$ (24), and finally dried again under a N_2 stream prior to overnight high vacuum. Lipids were dispersed in TBS and sonicated as described above. Titanium debris was removed by centrifugation (Marathon table centrifuge, Fisher Scientific), for 10 min at 12,000 rpm.

The binding of apoA-I to SUVs was analyzed by gel-permeation chromatography as described by Yokoyama et al. (35). To observe the interaction of vesicles with apoA-I, 0.93 mg of POPC in SUV were incubated for 1 h at room temperature with increasing concentrations of apoA-I (from 0.025 to 0.4 mg), in the lipid-free state, or reconstituted into 78 or 96 Å rHDL. The total volume of the reaction mixture was 0.5 ml. The reaction mixture was then applied to a small Sepharose CL-6B (1 × 5 cm) column, and 0.5 ml fractions were collected. The entire chromatographic elution was completed in 10 min. In each fraction, SUVs were detected by radioactivity and protein was determined by the fluorescamine assay (36). ApoA-I bound to vesicles (protein peak co-eluting with the liposomes) eluted separately from unbound protein (later fractions). Data were analyzed assuming a single set of binding sites and equilibrium conditions, according to equation 1 (35):

$$P_f = (N[PC]\ P_f / P_b) - K_d \qquad \textit{Eq. 1)}$$

where P_f is the concentration of free (unbound) protein, P_b is the concentration of bound protein, [PC] is the concentration of POPC in the reaction mixture, N is the binding stoichiometry (upper limit of $P_b/[PC]$), and K_d is the dissociation constant. The model assumes a finite number of discrete, equivalent, and non-interacting binding sites on the surface of the vesicles.

The VP-ITC microcalorimeter (MicroCal, Northampton, MA) was used to study the binding of apoA-I in the three physical states to SUVs. Typically 20 consecutive injections of 10 μl aliquots of the protein at a concentration of 30–110 μM were injected from the syringe into the cell (1.44 ml) containing 3–30 mM POPC solutions of SUVs. Injections were made at intervals of 10 min and the duration of each injection was according to the volume added (2 s/μl of injectant). To assure proper mixing after each injection, a constant stirring speed of 300 rpm was maintained during the experiment. The temperature in the cell was 30°C and lipid solutions were degassed under vacuum prior to use. Dilution heats of protein into the lipid solution were subtracted from measured heats of binding. These values agreed with those obtained in corresponding protein-buffer titrations. To ensure chemical equilibration, the protein solution was dialyzed against the same buffer as that of the POPC SUVs prior to the ITC experiments. Data were analyzed using the Origin software provided by Micro-Cal Inc.

ApoA-I (in lipid-free state or in 78 or 96 Å particles) was incubated with POPC SUVs in order to test its ability to rearrange to different-sized particles in the presence of excess phospholipids. Ten μl of apoA-I (12 μg) were incubated at room temperature with 5 μl of SUV (48 μg of POPC) for 0, 1, 2, 6, 14, and 24 h. Incubation was stopped by placing the samples on ice. Rearrangement was analyzed immediately by native (8–25%) polyacrylamide gradient gel electrophoresis. In a separate experiment, 10 μl of apoA-I (12 μg) were incubated with 5 μl of SUV containing different POPC concentrations, in order to reach a w/w ratio of 1, 2, 4, 8, and 16, POPC/apoA-I. Mixtures were incubated for 6 h and analyzed the same way as described above. The extent of particle rearrangement was determined by laser densitometry scanning of the gels stained with Coomasie Blue, on an LKB Ultroscan laser densitometer.

RESULTS

Reconstituted HDL, 78 Å and 96 Å in diameter, were prepared using different starting POPC/apoA-I ratios and were isolated as described in Materials and Methods. After isolation, samples were analyzed in terms of homogeneity, size, and lipid composition. Cross-linking and SDS-PAGE analysis revealed that both particles contained two molecules of apoA-I, and both preparations exhibited only one major band when analyzed by electrophoresis under native conditions confirming the homogeneity of the particles (**Fig. 1**).

From previous work, it is well known that the conformation of apoA-I is distinct in the lipid-free state and in these two species of rHDL particles (21, 37). Fluorescence and circular dichroism measurements on the current samples agreed well with published values and are listed in **Table 1**, together with previously published structural and functional parameters for the 78 Å and 96 Å particles. Compared with the larger 96 Å particles, apoA-I in the 78 Å species has a lower α-helix content, and lower apparent stability. On average, the negative charges contributed by the apoA-I in the 78 Å particles are fewer, and exposure of Trp residues to solvent is decreased. These conformational differences in apoA-I are dramatically reflected in the 16-fold lower activation of LCAT in the 78 Å particles and a 60-fold decreased affinity of the smaller particles for binding to SR-BI receptors.

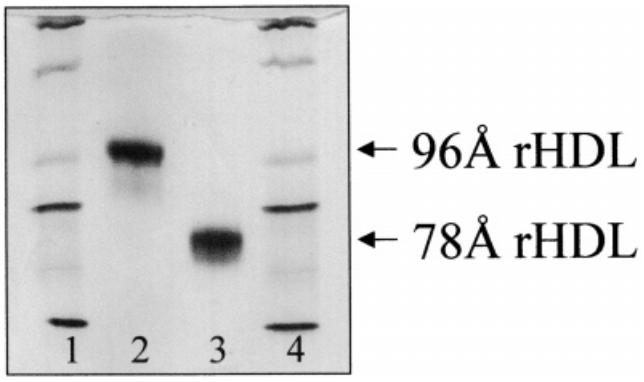

Fig. 1. Native 8–25% polyacrylamide gel of the rHDL complexes, stained with Coomasie Blue. Lanes 1 and 4 show high molecular weight markers (Amersham Pharmacia Biotech); lane 2 corresponds to the 96 Å rHDL, and lane 3 to the 78 Å rHDL.

TABLE 1. Structural and functional properties of lipid-free apoA-I and apoA-I in two defined rHDL

	Lipid-free ApoA-I	78 Å rHDL	96 Å rHDL
POPC/apoA-I (mol/mol)[a]	—	30 (± 3):1	68 (± 3):1
α-helix content (%)[b]	56 ± 5	61 ± 5	73 ± 8
ΔG^0 (kcal/mol)[c]	2.5 ± 0.1	1.8 ± 0.2	2.6 ± 0.9
WMF Trp (nm)[d]	334 ± 1	333 ± 1	333 ± 1
Valence (e)[e]	−3.2 ± 0.1	−6.1 ± 0.2	−7.5 ± 0.5
K_{sv} (M^{-1})[f]	6.9 ± 1.0	1.5 ± 0.2	3.7 ± 1.9
Reactivity with LCAT (nmol CE/h. M)[g]	—	3.1×10^4	50×10^4
Binding to SR-BI K_d (μg/ml)[h]	—	48	0.84

[a] Protein concentration was determined according to Markwell et al. (31); POPC content was measured by the procedure of Chen et al. (32).

[b] Obtained from molar ellipticities at 222 nm (20).The current values compare quite well with those determined by McGuire et al. (20).

[c] Standard free energies of denaturation determined by McGuire et al. (20) from circular dichroism measurements.

[d] Wavelength of maximum fluorescence of Trp residues.

[e] Excess of negative charge per particle in electronic units. Determined by agarose gel electrophoresis by McGuire et al. (20).

[f] Stern-Volmer constants indicating exposure of Trp residues to quenching by KI; determined by McGuire et al. (20).

[g] Reactivity with lecithin cholesterol acyltransferase is expressed as apparent V_{max}/apparent K_m; taken from Jonas et al. (21).

[h] Apparent dissociation constant for the specific binding of ^{125}I-rHDL to CHO cells expressing SR-BI; taken from de Beer et al. (22).

Interactions with GUVs

ApoA-I labeled with Alexa 488 was used in two-photon fluorescence microscopy visualization of the binding of lipid-free and lipid-bound apoA-I to GUVs. Alexa 488 is a highly fluorescent photostable probe with the spectral characteristics of fluorescein. Due to the high solubility of the probe in aqueous solutions, apoA-I is easily and specifically labeled. Previous work (38) indicated that the attachment of one molecule of an analogous Alexa 488 probe per molecule of a Cys mutant of apoA-I did not introduce modifications in the secondary structure nor in the lipid binding properties of this apolipoprotein. Even less perturbation is expected in the present case because native apoA-I is labeled at random Lys residues that are exposed to water. Reconstitution of both kinds of rHDL in high yields with the labeled protein confirmed that the lipid binding and folding properties of apoA-I are not affected (38). **Figure 2** shows the images of POPC GUVs after the addition of the lipid-free labeled apoA-I (Fig. 2A), the 96 Å rHDL (Fig. 2B), and 78 Å rHDL (Fig. 2C). Control images before the addition of the fluorescent molecules showed no fluorescence intensity. For each image in Fig. 2 we also show the horizontal intensity profile taken in the region indicated by the white dashed line in the image. A peak in the average intensity around pixel 150 indicates protein bound to the GUV surface, when incubated with apoA-I in the lipid-free state or in 78 Å rHDL

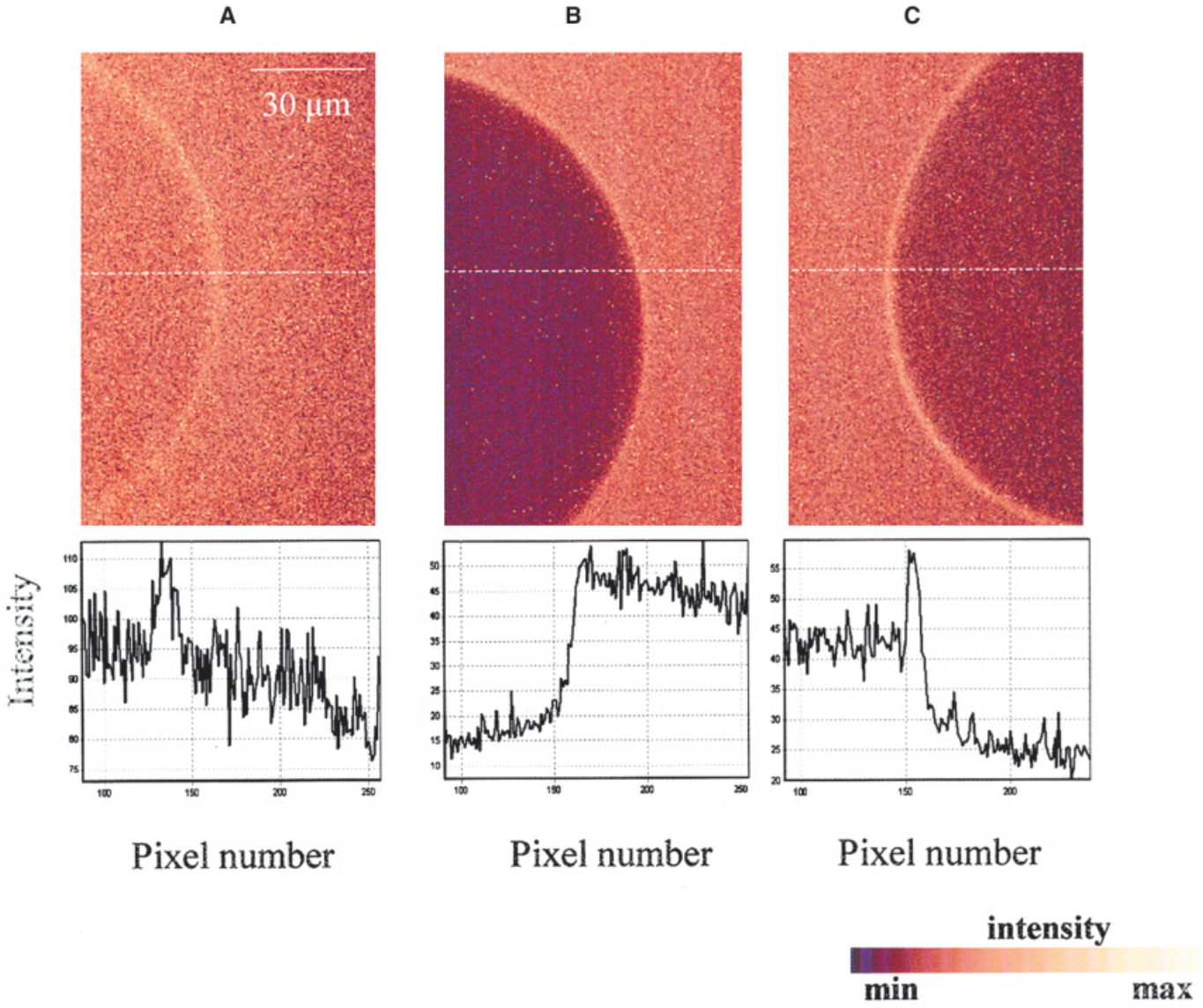

Fig. 2. Two-photon fluorescence microscopy images of POPC GUVs at 25°C in 1 mM Tris pH 8.0, 30 min after the addition of Alexa 488-labeled lipid-free apoA-I (A), 96Å rHDL (B), and 78 Å rHDL particles (C). Images correspond to the integration of 80 scans. The white dashed line shows the points where the horizontal intensity profiles (pictured under each image) were analyzed. Images were taken in the center of the GUVs. The relative fluorescence intensities are represented by the color palette shown below.

(Fig. 2A and 2C). The area below the peak indicates that, under the same conditions, the lipid-free protein binds with an affinity ~3 times higher than the 78 Å rHDL. For the 96 Å particles (Fig. 2B) binding was not detected by this criterion.

To observe the effects of apoA-I in the three conformational states on the structures and lipid content of the GUVs, unlabeled apoA-I species were added to GUVs doped with LAURDAN. Changes in the vesicle fluorescence, after the addition of apoA-I, were followed for about 2 h (**Fig. 3**). The first (left) panel in each figure shows the vesicles before the addition of apoA-I in the three conformational states. No detectable changes were observed when GUVs were incubated with either lipid-free apoA-I or with 96Å rHDL (Fig. 3A and 3B, respectively). However, when the 78 Å rHDL were added to the vesicles, two main changes were detected: *1*) after about 30 min, deformation of vesicles was frequently observed, together with an increase in the background fluorescence (Fig. 3C, center), and *2*) after approximately 1.5 h the same vesicle becomes round again, but it has some surface features (Fig. 3C, boxed). A closer look at this vesicle (Fig. 3C, zoom) shows a "network-like" structure of uneven lipid distribution. The increase in the background fluorescence could be attributed to probe molecules that were present in solution and became fluorescent when they partitioned into the 78 Å rHDL. However, a similar effect was not observed for the 96 Å rHDL, eliminating that possibility. Apparently LAURDAN and, most likely POPC molecules, are removed from the GUVs by specific interaction with the 78 Å rHDL only.

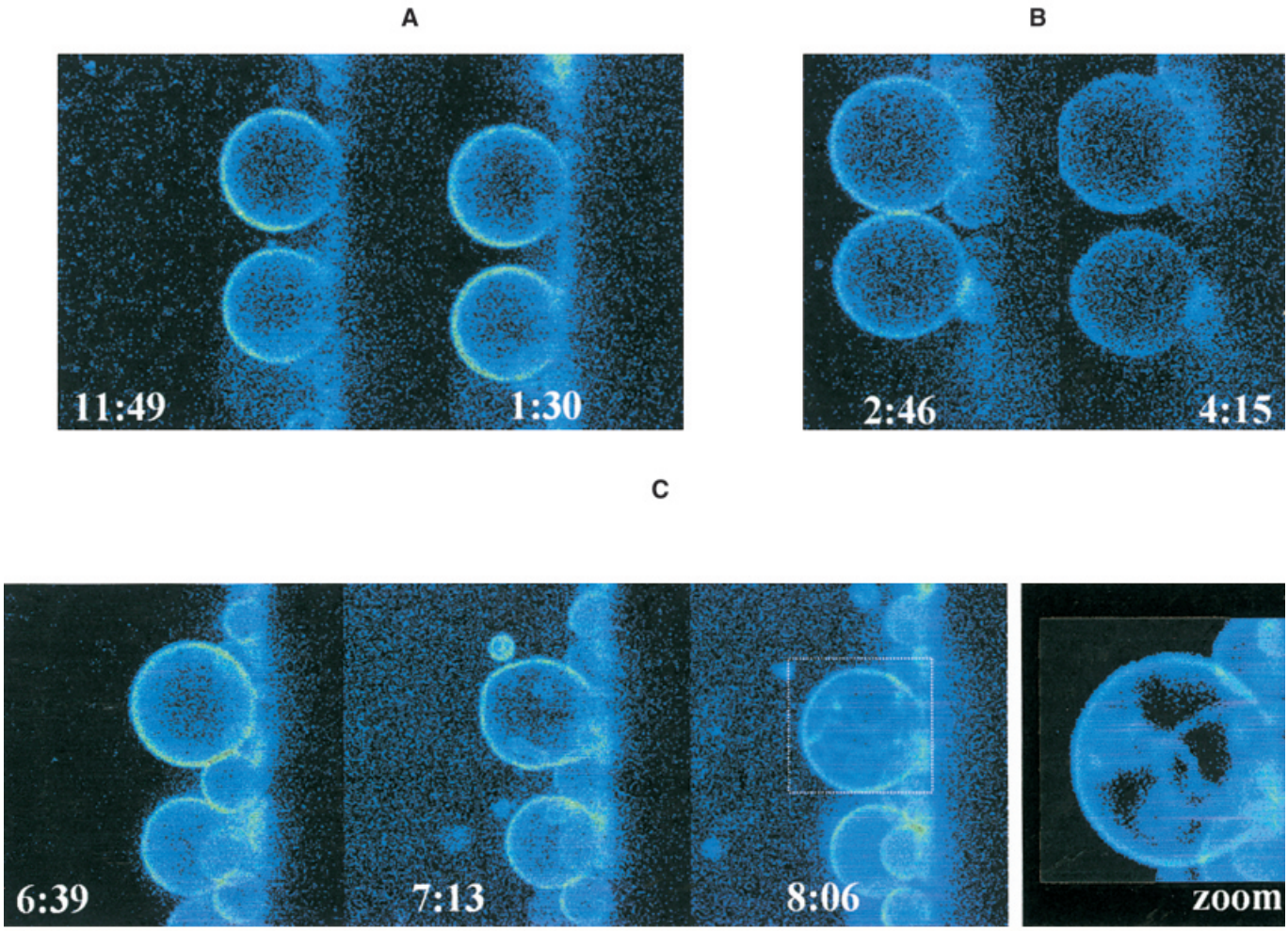

Fig. 3. Two-photon fluorescence microscopy images of POPC GUVs doped with LAURDAN after the addition of unlabeled lipid-free apoA-I (A), 96Å rHDL (B), and 78 Å rHDL particles (C). Incubation conditions are described in the Materials and Methods. Images were taken in the center of the GUVs.

Interactions with SUV

In order to compare the affinity of the different apoA-I species for POPC bilayers, binding of apoA-I to POPC SUVs was analyzed by the gel-permeation method (35). The binding curves for the apoA-I in the different conformations are shown in **Fig. 4**. Bound protein at each concentration was determined from the area of protein co-eluting with the vesicles. In good agreement with Yokoyama et al. (35), the association of the lipid-free apoA-I was rapid and reached saturation under the conditions of the experiment. A weaker binding was detected for the 78 Å rHDL. Binding parameters were also obtained by ITC (39). A typical calorimetric titration pattern is shown in **Fig. 5**. Experimental data were fitted using a Langmuir adsorption model to obtain dissociation constants (K_d) and binding capacity values (r). Both sets of binding parameters are listed in **Table 2**. A correction was applied to the POPC concentration to account for the fact that the protein binds only to the external leaflet that represents about 60% of the total lipids of the SUV. Binding of 96 Å rHDL to SUVs was not observed by the gel-permeation or by the ITC method. Binding of lipid-free apoA-I occurred with high affinity and gave comparable equilibrium dissociation constants (K_d) and stoichiometries (POPC/apoA-I = r) with both methods. Assuming that the average SUV has about 3,000 POPC molecules with 60% in the outer leaflet and accessible to apoA-I, then it can be calculated that two molecules of apoA-I are bound per vesicle at saturation.

Binding of the 78 Å rHDL to SUVs was measured by both methods, and it was found to be weaker than the binding of lipid-free apoA-I. However, the numerical agreement between both methods was poor. This discrepancy may be attributed to the intrinsic limitations of the measurements. In the gel-permeation method, the column separation of lipid-bound and free protein may perturb equilibrium especially for lower affinity interactions. In contrast, the ITC measurements are performed under equilibrium conditions, and the relative affinity observed for the lipid-free apoA-I and the 78 Å particles (around three-fold higher for the lipid-free state) is in good agreement with the results obtained from the two-photon microscopic binding experiments. Also, the gradual remodeling that the 78 Å rHDL undergo during the course of the binding experiments (to larger rHDL with lower affinity

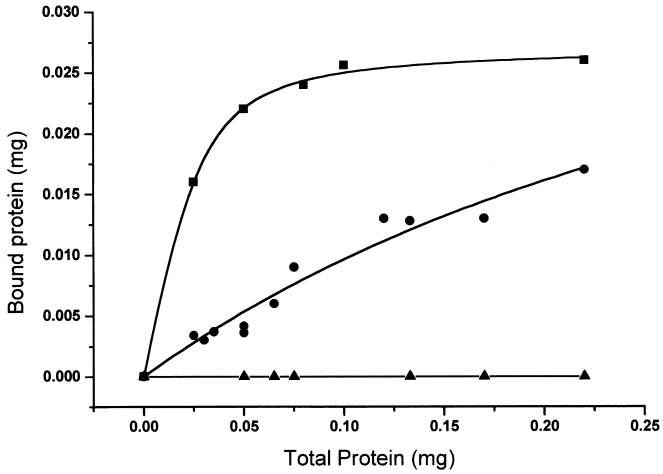

Fig. 4. Binding curves of the different conformational states of apoA-I to small unilamellar vesicles using the gel-permeation method (35). Isotherms were measured as described in Materials and Methods. A constant amount of POPC (0.93 mg) was incubated with increasing amounts of apoA-I. Squares correspond to lipid-free apoA-I, circles to 78 Å rHDL, and triangles to 96 Å rHDL. Solid lines are the theoretical Langmuir isotherms calculated from equation 1. The model assumes binding sites to be independent and identical.

for the SUV, see the next section) could affect the outcome of the experiments depending on temperature, reagent concentrations, and the time it takes to perform the experiment. At the same time, the vesicle properties are also changing because of phospholipid depletion. In spite of these concerns, the binding constants obtained within 1–2 h from mixing of the reactants, under the general conditions of our experiments, should give a reasonable indication of the relative affinities of apoA-I in the different conformations for the POPC vesicles. The stoichiometry of binding of the 78 Å rHDL obtained by the ITC method suggests that the surface area occupied by each of these particles on the SUVs is considerably smaller than that occupied by the lipid-free apoA-I. This agrees with the hypothesis that, in contrast to lipid-free apoA-I, which has eight helical repeats available for binding, the 78 Å rHDL have two helical repeats per apoA-I that can bind to SUV surfaces.

In order to obtain more information about the process occurring on the surface of the GUVs, we analyzed the ability of apoA-I to solubilize POPC in the presence of excess SUV. ApoA-I species (lipid-free and the two rHDL particles) were incubated with POPC SUVs at room temperature, for various time periods, and at different SUV/protein ratios, and the products were analyzed by native gradient gel electrophoresis (**Fig. 6**). Neither lipid-free apoA-I nor the 96 Å rHDL showed any differences in electrophoretic migration or particle distribution with respect to the samples incubated in the absence of SUV, indicating that net lipid transfers did not occur in these samples after 6 h of incubation with increasing amounts of SUVs (Fig. 6A). In contrast, the 78 Å rHDLs were remodeled into larger particles, predominantly particles with 96 Å diameters. About 5, 18, 24, 33, and 56% of the protein in

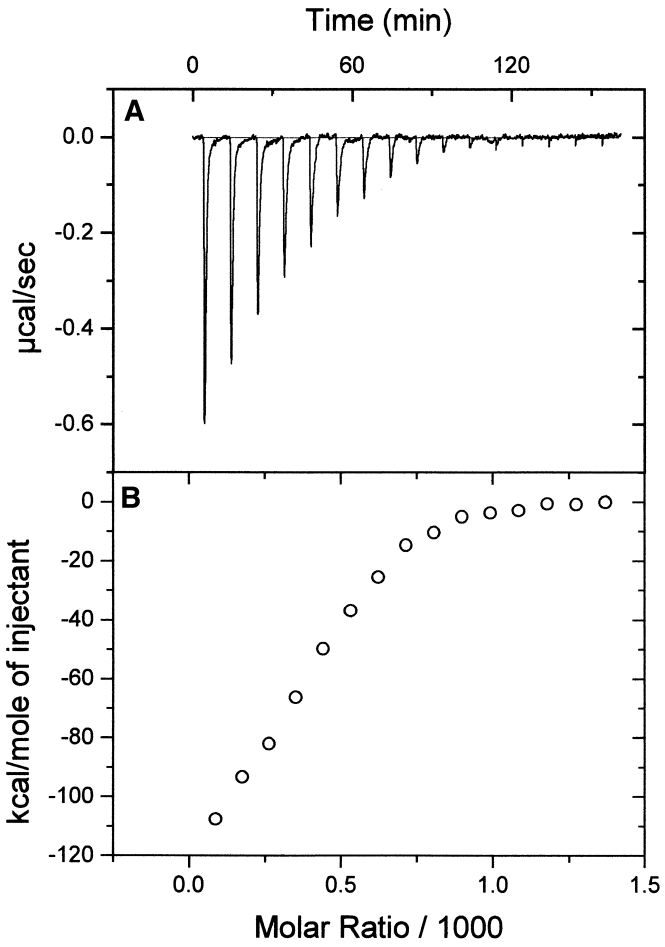

Fig. 5. Binding of lipid-free apoA-I to SUV measured by isothermal titration calorimetry. Ten µl of apoA-I (36 µM) were injected each time at intervals of 10 min into the cell containing 2.9 mM POPC SUVs in TBS at 30°C. Baseline was corrected substracting the heat of dilution. A: Each peak represents the heat absorbed when binding occurs after each injection. B: Normalized binding enthalpies as a function of the injection number. K_d and r values were obtained from the fit of the experimental data.

the original 78 Å rHDL particles appeared in bigger complexes when incubated with 1, 2, 4, 8, and 16 w/w excess SUV lipid to apoA-I, respectively. Remodeling of a small

TABLE 2. Binding parameters for apoA-I in the lipid-free state and in 78 Å rHDL to small unilamellar vesicles, determined from Isothermal Titration Calorimetry (ITC) and Gel-Permeation Chromatography (GPC)

	Lipid-Free ApoA-I		78 Å rHDL	
	ITC	GPC	ITC	GPC
K_d (µM)[a]	0.25 ± 0.06	0.40 ± 0.03	0.86 ± 0.30	15.5 ± 2.20
N (mmol protein/mol POPC)[b]	0.64 ± 0.1	1.30 ± 0.10	2.20 ± 0.20	1.30 ± 0.10
r (mol POPC/mol protein)[c]	937	461	273	461

[a] Dissociation constant.
[b] Stoichiometry of binding of the protein to the lipid vesicles.
[c] Binding capacity (1/N) is the size of the binding site considering only the phospholipids in the external leaflet of the vesicle (60% of the total concentration).

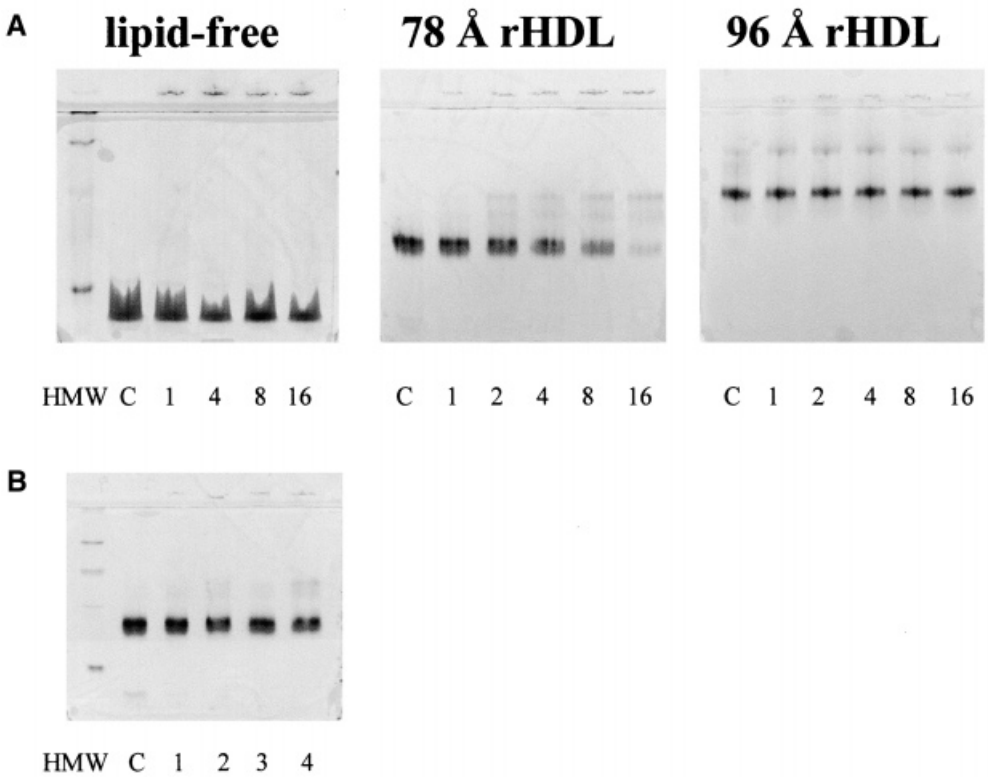

Fig. 6. Nondenaturing electrophoretic analysis of the rearrangement of particles exposed to an excess of POPC SUVs. Gels were stained with Coomasie Blue and scanned to quantify the protein in the bands. A: ApoA-I in different conformational states was incubated for 6 h at room temperature with increasing amounts of POPC; HMW, molecular weight standard markers (Amersham Pharmacia), c, control of the apoA-I or rHDL incubated for 6 h without SUVs. The numbers under each lane represent the mass ratios of POPC/apoA-I used in each incubation. B: Short term incubation of the 78 Å rHDL with SUVs. Lanes 1 and 2 show a 1 min incubation at weight ratios of 2 and 4 POPC/apoA-I, respectively. Lanes 3 and 4 show a one-hour incubation at the same weight ratios of POPC/apoA-I.

proportion of particles was observed even at short times of incubation (Fig. 6B), comparable to the observation time at the microscope (1–2 h). No lipid-free apoA-I was produced as a result of the remodeling of these particles.

DISCUSSION

In this study we demonstrated that three different conformations of apoA-I regulate their binding to phospholipid vesicle membranes and the abstraction of lipids from them. Similar conformational adaptations of apoA-I are most likely responsible for the different functional roles of native HDL subclasses in reverse cholesterol transport.

The three well-defined structural forms of apoA-I employed in this study were the lipid-free form and the lipid-bound states associated with the 78 Å and 96 Å rHDL particles, which differ from each other in apoA-I conformation, phospholipid content, and functional roles in LCAT activation (21) and binding to SR-BI receptors (22). In addition, the 78 Å and 96 Å rHDL resemble the native preβ-HDL subclasses that contain only apoA-I, have high proportions of phospholipid relative to other lipids, and have predominantly discoidal shapes. The best studied preβ_1-HDL particles appear to have intermediate properties between lipid-free apoA-I and the synthetic 78 Å rHDL species. Several reports indicate that preβ_1-HDL, the initial acceptors of cholesterol from cell membranes (14), have a molecular mass around 70 kDa, 2 apoA-I molecules per particle, up to 20 molecules of phospholipid, and very few molecules of cholesterol ester (40). The conformation of apoA-I in these particles is distinct from apoA-I in other HDL subclasses as revealed by epitope accessibility (41) and exposure of the central region to proteolytic digestion (42). Structural information is scarce on the larger preβ-HDL (preβ_3-HDL), but in their discoidal shape, high content of phospholipids, and optimal efficiency as LCAT substrates, these particles do resemble the 96 Å rHDL used in this study.

In contrast to the limited information available about the conformation of apoA-I in the preβ-HDL particles, the structures of lipid-free apoA-I and of apoA-I in the 78 Å and 96 Å rHDL particles have been studied in some detail. Monomeric, lipid-free apoA-I in physiological buffers has the characteristics of a molten globule (43) and contains about 50% α-helical structure, folded in an elongated hairpin that brings the compact N- and C-terminal ends

near to each other (44). In the rHDL particles, apoA-I acquires more α-helical structure and the amphipathic helical segments of the two apoA-I molecules are directly involved in binding to phospholipid (POPC) acyl chains. Fewer helices are required to cover the periphery of the smaller 78 Å rHDL discs than of the larger 96 Å particles. In the 96 Å rHDL, all of the amphipathic helices encoded by exon 4 are engaged in interactions with POPC molecules.

The three-dimensional arrangement of apoA-I helices in rHDL particles has been modeled by Phillips et al. (45) and by Segrest et al. (46). Although they differ in the orientation of the helix axes and apoA-I monomer-to-monomer contacts, both models predict maximal α-helical structure (75–80%) and maximal contacts with phospholipid acyl chains. Most recently, based on extensive fluorescence resonance energy transfer experiments, we suggested a hairpin fold of each apoA-I monomer in the 96 Å particles (38). Again, in this model all the helical segments are involved in lipid-binding, but the central helices, at the hairpin turn, could easily disengage from the lipid surface to effect the rearrangement required for the reversible transformation of 96 Å rHDL into 78 Å rHDL particles. The precise helical repeats that are disrupted in the 78 Å rHDL are not known, but central helices toward the N-terminus are strongly suggested by several lines of evidence. The hinge or mobile region of apoA-I has been localized between residues 99 and 143 of the sequence (47), the same region that is accessible to proteases in preβ_1-HDL particles (42). Furthermore, the properties of Trp residues are affected in the 78 Å particles, suggesting an involvement of Trp 108 in the conformational adaptations of apoA-I. Corsico et al. (48) have implicated residues 87–112 of apoA-I in their recent study of interactions of rHDL with membranes. However, in contrast to the present work, Corsico et al. did not distinguish between rHDL subclasses. Thus, having apoA-I in three well-defined conformations, we set out to study their effects on apoA-I interactions with POPC membranes.

First, we confirmed the essentially reversible binding of lipid-free apoA-I to SUVs at high POPC to apoA-I ratios and periods of 2 h or less of incubation. The conventional gel-permeation method (35) was supported by two novel approaches: isothermal titration microcalorimetry and two-photon fluorescence microscopic visualization. In addition, we demonstrated that lipid-free apoA-I, under these conditions, abstracts little or no lipid from the POPC membranes, so that vesicle structure is not perturbed and rHDL particles are not formed; this was shown by the unchanged GUV structure, absence of LAURDAN fluorescence in the background, and apoA-I remaining at the lipid-free migration position on the native gels. Under different conditions, where complex cell membranes are used, prolonged incubation times and high apolipoprotein concentrations, some membrane solubilization has been reported (49). However, under the precisely controlled conditions of these experiments, it is clear that lipid-free apoA-I binds with high affinity to POPC membranes but does not disrupt them, nor does it solubilize significant amounts of lipid.

Comparison of the two kinds of rHDL particles in their binding to SUVs and GUVs clearly shows that the smaller particles have measurable binding affinity for both of these vesicles systems, whereas the 96 Å species shows little or no binding. This difference in binding behavior can be explained by the different apoA-I conformation in both types of particles. In the 96 Å rHDL, the apoA-I helical segments are all involved in lipid binding within the rHDL, whereas in the 78 Å rHDL, each apoA-I has a region that is available for amphipathic helix formation and binding to phospholipid membranes.

Compared with lipid-free apoA-I binding to SUVs, the affinity of the 78 Å rHDL is lower and the POPC/apoA-I (r value) is also lower, in agreement with the hypothesis that only about two helical repeats per apoA-I (four per particle) are involved in the binding of the 78 Å rHDL to the membranes. The nature of this interaction apparently favors the desorption of phospholipids and LAURDAN from the membrane and their solubilization in the rHDL particles. This is manifested by the appearance of LAURDAN fluorescence in the medium and morphological changes in the GUVs in the presence of the 78 Å particles. Also, exposure to SUVs results in the remodeling of the 78 Å rHDL into larger rHDL, including 96 Å species. This rearrangement occurs by the uptake of POPC from the vesicles. Thus, the 78 Å and 96 Å rHDL are interconvertible depending on the direction of phospholipid movement. The 78 Å rHDL are readily formed from 96 Å rHDL when these particles are depleted of phospholipid [for example upon incubation with LDL (50)]; and 96 Å rHDL are formed from the 78 Å rHDL by lipid uptake from phospholipid vesicles, as demonstrated in this study.

The conformational changes in apoA-I that occur in conjunction with the changes in phospholipid content of the rHDL also lead to major functional switches: *1*) changes in the affinity for the phospholipid membranes, as demonstrated here, *2*) dramatic changes in LCAT activation (21), and *3*) very marked changes in affinity for the SR-BI receptors (22).

In summary, the 78 Å rHDL bind to the vesicles, abstract POPC and are converted into 96 Å particles that no longer bind to the vesicles but are excellent substrates for LCAT (after incorporation of cholesterol) and are good ligands for SR-BI receptors in contrast to the 78 Å particles.

The metabolic steps outlined above for the in vitro system are very plausible in vivo in RCT. The preβ_1-HDL, if they have a favorable apoA-I conformation similar to the 78 Å rHDL, may interact with and abstract membrane lipids (phospholipids and cholesterol) from cells. In its original state, preβ_1-HDL would not be a good substrate for LCAT, or an efficient ligand for SR-BI receptors. After enrichment with phospholipids, the structure of apoA-I would switch to a form that no longer binds to membrane lipids, but can effectively activate LCAT and bind to SR-BI receptors. Subsequent steps of facilitated transfers of phospholipids to LDL and other lipoproteins, continued LCAT activity, and hepatic lipase action would deplete the mature HDL of phospholipids, leading to particle rearrangements

that must certainly involve one or more conformational switches in apoA-I.

The reported interaction of lipid-free apoA-I with the ABC1 transporter (8) and energy-dependent transfer of cellular lipids to apoA-I may represent the initial lipidation of apoA-I to form preβ_1-HDL particles, or it could be a separate pathway for lipid efflux from cells. In any event, the conformational adaptability of apoA-I is not only a mechanism by which the apolipoprotein adjusts to different lipid loads, but also constitutes a molecular switch for turning on and off key functions of apoA-I in HDL: binding to phospholipid membranes and lipid uptake, LCAT activation, and SR-BI receptor binding.

The authors thank Dr. Timothy Shedd for his help in the design and construction of the chamber for fluorescence microscopy. This work was supported by National Institutes of Health grants RR-03155 to E.G. and NIH grant HL-16059 to A.J.

Manuscript received 2 August 2001 and in revised form 16 October 2001.

REFERENCES

1. Miller, G. J., and N. E. Miller. 1975. Plasma-high-density-lipoprotein concentration and development of ischaemic heart-disease. *Lancet.* **1:** 16–19.
2. Goldbourt, U., S. Yaari, and J. H. Medalie. 1997. Isolated low HDL cholesterol as a risk factor for coronary heart disease mortality: A 21-year follow-up of 8000 men. *Arterioscler. Thromb. Vasc. Biol.* **17:** 107–113.
3. Fournier, N., V. Atger, J. L. Paul, M. D. L. Moya, G. Rothblat, and N. Moatti. 1999. Fractional efflux and net change in cellular cholesterol content mediated by sera from mice expressing both human apolipoprotein AI and human lecithin: cholesterol acyltransferase genes. *Atherosclerosis.* **147:** 227–235.
4. Johnson, W. J., F. H. Mahlberg, G. H. Rothblat, and M. C. Phillips. 1991. Cholesterol transport between cells and high-density lipoproteins. *Biochim. Biophys. Acta.* **1085:** 273–298.
5. Fielding, C. J., and P. E. Fielding. 1995. Molecular physiology of reverse cholesterol transport. *J. Lipid Res.* **36:** 211–228.
6. Fielding, C. J., V. G. Shore, and P. E. Fielding. 1972. A protein cofactor of lecithin:cholesterol acyltransferase. *Biochem. Biophys. Res. Commun.* **46:** 1493–1498.
7. Oram, J. F., and S. Yokoyama. 1996. Apolipoprotein-mediated removal of cellular cholesterol and phospholipids. *J. Lipid Res.* **37:** 2473–2491.
8. Wang, N., D. L. Silver, P. Costet, and A. R. Tall. 2000. Specific binding of apoA-I, enhanced cholesterol efflux, and altered plasma membrane morphology in cells expressing ABC1. *J. Biol. Chem.* **275:** 33053–33058.
9. Acton, S., A. Rigotti, K. T. Landschulz, S. Xu, H. H. Hobbs, and M. Krieger. 1996. Identification of scavenger receptor SR-BI as a high density lipoprotein receptor. *Science.* **271:** 518–520.
10. Silverman, D. I., G. S. Ginsburg, and R. C. Pasternak. 1993. High-density lipoprotein subfractions. *Am. J. Med.* **94:** 636–645.
11. Brouillette, C. G., and G. M. Anantharamaiah. 1995. Structural models of human apolipoprotein A-I. *Biochim. Biophys. Acta.* **1256:** 103–129.
12. Rye, K-A., and M. N. Duong. 2000. Influence of phospholipid depletion on the size, structure, and remodeling of reconstituted high density lipoproteins. *J. Lipid Res.* **41:** 1640–1650.
13. Lefevre, M., C. H. Sloop, and P. S. Roheim. 1988. Characterization of dog prenodal peripheral lymph lipoproteins. Evidence for the peripheral formation of lipoprotein-unassociated apoA-I with slow pre-beta electrophoretic mobility. *J. Lipid Res.* **29:** 1139–1148.
14. Castro, G. R., and C. J. Fielding. 1988. Early incorporation of cell-derived cholesterol into pre-beta-migrating high-density lipoprotein. *Biochemistry.* **27:** 25–29.
15. Francone, O. L., A. Gurakar, and C. J. Fielding. 1989. Distribution and functions of lecithin:cholesterol acyltransferase and cholesteryl ester transfer protein in plasma lipoproteins. Evidence for a functional unit containing these activities together with apolipoproteins A-I and D that catalyzes the esterification and transfer of cell-derived cholesterol. *J. Biol. Chem.* **264:** 7066–7072.
16. Francone, O. L., and C. J. Fielding. 1990. Initial steps in reverse cholesterol transport: the role of short-lived cholesterol acceptors. *Eur. Heart J.* **Suppl. E:** 218–224.
17. Xu, S., M. Laccotripe, X. Huang, A. Rigotti, V. I. Zannis, and M. Krieger. 1997. Apolipoproteins of HDL can directly mediate binding to the scavenger receptor SR-B1, an HDL receptor that mediates selective lipid uptake. *J. Lipid Res.* **38:** 1289–1298.
18. Ji, Y., B. Jian, N. Wang, Y. Sun, M. de la Llera Moya, M. C. Phillips, G. H. Rothblat, J. B. Swaney, and A. R. Tall. 1997. Scavenger receptor BI promotes high density lipoprotein-mediated cellular cholesterol efflux. *J. Biol. Chem.* **272:** 20982–20985.
19. Patsch, J. R., and A. M. J. Gotto. 1987. Metabolism of high density lipoproteins. *In*: Plasma Lipoproteins. A. M. J. Gotto, editor. Elsevier, Amsterdam. 221–250.
20. McGuire, K. A., W. S. Davidson, and A. Jonas. 1996. High yield overexpression and characterization of human recombinant proapolipoprotein A-I. *J. Lipid Res.* **37:** 1519–1528.
21. Jonas, A., J. H. Wald, K. L. Toohill, E. S. Krul, and K. E. Kezdy. 1990. Apolipoprotein A-I structure and lipid properties in homogeneous, reconstituted spherical and discoidal high density lipoproteins. *J. Biol. Chem.* **265:** 22123–22129.
22. de Beer, M. C., D. M. Durbin, L. Cai, A. Jonas, F. C. de Beer, and D. R. van der Westhuyzen. 2001. Apolipoprotein A-I conformation markedly influences HDL interaction with scavenger receptor B1. *J. Lipid Res.* **42:** 309–313.
23. Huang, C-H. 1969. Studies on phosphatidylcholine vesicles. Formation and physical characteristics. *Biochemistry.* **8:** 344–351.
24. Breukink, E., P. Ganz, B. de Kruijff, and J. Seelig. 2000. Binding of nisin Z to bilayer vesicles as determined with isothermal titration calorimetry. *Biochemistry.* **39:** 10247–10254.
25. Pownall, H. J., Q. Pao, D. Hickson, J. T. Sparrow, S. K. Kusserow, and J. B. Massey. 1981. Kinetics and mechanism of association of human plasma apolipoproteins with dimyristoylphosphatidylcholine: effect of protein structure and lipid clusters on reaction rates. *Biochemistry.* **20:** 6630.
26. Menger, F. M., and J. S. Keiper. 1998. Chemistry and physics of giant vesicles as biomembrane models. *Curr. Opin. Chem. Biol.* **2:** 726–732.
27. So, P. T. C., T. French, W. M. Yu, K. M. Berland, C. Y. Dong, and E. Gratton. 1995. Time resolved fluorescence microscopy using two-photon excitation. *Bioimaging.* **3:** 49–63.
28. Leroy, A., and A. Jonas. 1994. Native-like structure and self-association behavior of apolipoprotein A-I in a water/n-propanol solution. *Biochim. Biophys. Acta.* **1212:** 285–294.
29. Haugland, R. P. 1996. Handbook of fluorescent probes and research chemicals. 6th ed. Molecular Probes, Eugene, OR. 55–58.
30. Jonas, A. 1986. Reconstitution of high-density lipoproteins. *Methods Enzymol.* **128:** 553–582.
31. Markwell, M. A. K., S. M. Haas, L. L. Bieber, and N. E. Tolbert. 1978. A modification of the Lowry procedure to simplify protein determination in membrane and lipoprotein samples. *Anal. Biochem.* **87:** 206–210.
32. Chen, P. S., T. Toribara, and H. Warner. 1956. Microdetermination of phosphorous. *Anal. Chem.* **28:** 1756–1758.
33. Leroy, A., K. L. Toohill, J. C. Fruchart, and A. Jonas. 1993. Structural properties of high density lipoprotein subclasses homogeneous in protein composition and size. *J. Biol. Chem.* **268:** 4798–4805.
34. Bagatolli, L. A., and E. Gratton. 1999. Two photon fluorescence microscopy observation of shape changes at the phase transition in phospholipid giant unilamellar vesicles. *Biophys. J.* **77:** 2090–2101.
35. Yokoyama, S., D. Fukushima, J. P. Kupferberg, F. J. Kezdy, and E. T. Kaiser. 1980. The mechanism of activation of lecithin:cholesterol acyltransferase by apolipoprotein A-I and an amphiphilic peptide. *J. Biol. Chem.* **255:** 7333–7339.
36. Funk, G. M., C. E. Hunt, D. E. Epps, and P. K. Brown. 1986. Use of a rapid and highly sensitive fluorescamine-based procedure for the assay of plasma lipoproteins. *J. Lipid Res.* **27:** 792–795.
37. Bergeron, J., P. G. Frank, D. Scales, Q-H. Meng, G. Castro, and Y. L. Marcel. 1995. Apolipoprotein A-I conformation in reconstituted discoidal lipoproteins varying in phospholipid and cholesterol content. *J. Biol. Chem.* **270:** 27429–27438.

38. Tricerri, M. A., A. K. Behling Agree, S. A. Sanchez, J. Bronski, and A. Jonas. 2001. Arrangement of apolipoprotein A-I in reconstituted high density lipoprotein disks: an alternative model based on fluorescence resonance energy transfer experiments. *Biochemistry.* **40:** 5065–5074.
39. Wiseman, T., S. Williston, J. F. Brandts, and L. N. Lin. 1989. Rapid measurement of binding constants and heats of binding using a new titration calorimeter. *Anal. Biochem.* **179:** 131–137.
40. Kunitake, S. T., K. J. La Sala, and J. P. Kane. 1985. Apolipoprotein A-I-containing lipoproteins with pre-beta electrophoretic mobility. *J. Lipid Res.* **26:** 549–555.
41. Fielding, P. E., M. Kawano, A. L. Catapano, A. Zoppo, S. Marcovina, and C. J. Fielding. 1994. Unique epitope of apolipoprotein A-1 expressed in pre-beta-1 high-density lipoprotein and its role in the catalyzed efflux of cellular cholesterol. *Biochemistry.* **33:** 6981–6985.
42. Kunitake, S. T., G. C. Chen, S-F. Kung, J. W. Schilling, D. A. Hardman, and J. P. Kane. 1990. Pre-beta high density lipoprotein. Unique disposition of apolipoprotein A-I increases susceptibility to proteolysis. *Arterioclerosis.* **10:** 25–30.
43. Gursky, O., and D. Atkinson. 1996. Thermal unfolding of human high-density apolipoprotein A-1 .Implications for a lipid-free molten globule state. *Proc. Natl. Acad. Sci. USA.* **93:** 2991–2995.
44. Tricerri, M. A., A. K. Behling Agree, S. A. Sanchez, and A. Jonas. 2000. Characterization of apolipoprotein A-I structure using a cysteine-specific fluorescence probe. *Biochemistry.* **39:** 14682–14691.
45. Phillips, J. C., W. Wriggers, Z. G. Li, A. Jonas, and K. Schulten. 1997. Predicting the structure of a apolipoprotein A-1 in reconstituted high-density lipoprotein disks. *Biophys. J.* **73:** 2337–2346.
46. Segrest, J. P., M. K. Jones, A. E. Klon, C. J. Sheldahl, M. Hellinger, H. De Loof, and S. C. Harvey. 1999. A detailed molecular belt model for apolipoprotein A-I in discoidal high density lipoprotein. *J. Biol. Chem.* **274:** 31755–31758.
47. Calabresi, L., Q. H. Meng, G. R. Castro, and Y. L. Marcel. 1993. Apolipoprotein A-I conformation in discoidal particles. Evidence for alternate structures. *Biochemistry.* **32:** 6477–6484.
48. Corsico, B., J. D. Toledo, and H. A. Garda. 2001. Evidence for a central apolipoprotein A-I domain loosely bound to lipids in discoidal lipoproteins that is capable of penetrating the bilayer of phospholipid vesicles. *J. Biol. Chem.* **276:** 16978–16985.
49. Forte, T. M., R. Goth-Goldstein, R. W. Nordhausen, and M. R. McCall. 1993. Apolipoprotein A-I-cell membrane interaction: extracellular assembly of heterogeneous nascent HDL particles. *J. Lipid Res.* **34:** 317–324.
50. Jonas, A., K. E. Kezdy, and J. H. Wald. 1989. Defined apolipoprotein A-I conformations in reconstituted high density lipoprotein discs. *J. Biol. Chem.* **264:** 4818–4824.